10.1098/rsta.2004.1438

THE ROYAL SOCIETY

Carbon nanotube electron sources and applications

By Niels de Jonge[1] and Jean-Marc Bonard[2]†

[1]*Philips Research, Prof. Holstlaan 4, 5656 AA Eindhoven, The Netherlands* (niels.de.jonge@philips.com)

[2]*Institute for Nanostructure Physics, Ecole Polytechnique Fédérale de Lausanne, 1015 Lausanne EPFL, Switzerland*

Published online 18 August 2004

In this review we give an overview of the present status of research on carbon nanotube (CNT) field emitters and their applications. Several different construction principles of field-emission devices with CNTs are summarized. The emission mechanism is introduced and a detailed overview is given of the measured emission properties and related topics of CNT electron sources. We give also several examples of field-emission devices with CNT electron emitters that are presently being investigated in the academic world as well as in industry. Carbon nanotube electron sources clearly have interesting properties, such as low voltage operation, good stability, long lifetime and high brightness. The most promising applications are the field-emission display and high-resolution electron-beam instruments. But several hurdles remain, such as the manufacture of an electron source or an array of electron sources with exactly the desired properties in a reproducible manner.

Keywords: carbon nanotubes; field emission; display; electron microscope; X-ray source; field emission lamp

1. Introduction

In 1995, four years after the discovery of carbon nanotubes (CNTs) by Iijima (1991), three groups reported field emission from CNTs at low-turn-on fields and high current densities (Chernozatonskii *et al*. 1995; de Heer *et al*. 1995; Rinzler *et al*. 1995). From 1998 on, the perspective to use nanotubes in field-emission devices spurred on efforts worldwide: a first display (Wang *et al*. 1998) as well as a lighting element (Jung *et al*. 2001; Saito & Uemura 2000) were presented. The field has been experiencing a rapid growth the past few years, and it is encouraging to note that two commercial products, namely high-brightness luminescent elements and an X-ray tube, have hit the market. Applications such as flat displays (Choi *et al*. 1999; Jung *et al*. 2001; Wang *et al*. 2001), cathode-ray lamps (Saito & Uemura 2000), X-ray-tube sources (Sugie *et al*. 2001; Yue *et al*. 2002), electron sources for high-resolution electron-beam instruments such as electron-beam lithography (EBL) machines and electron microscopes (Bonard *et al*. 1999; de Jonge *et al*. 2002) are under active consideration.

† Present address: Rolex SA, 3–7 rue Francois-Dussaud, 1211 Geneva 24, Switzerland.

One contribution of 12 to a Theme 'Nanotechnology of carbon and related materials'.

Carbon nanotubes have several advantages over other field-emitting materials. In contrast to commonly used emitters such as tungsten, a nanotube is not a metal, but a structure built by covalent bonds. A single-walled CNT is a graphite sheet that is rolled into a cylinder of a few micrometres in length and a few nanometres in diameter. A multi-walled nanotube (MWNT) consists of several such cylinders nested inside each other. Each carbon atom is bound to three other carbon atoms by a (covalent) sp^2 bond. As a result, the activation energy for surface migration of the emitter atoms is much larger than for a tungsten electron source. Therefore, the tip can withstand the extremely strong fields (several $V\,nm^{-1}$) needed for field emission. Depending on the exact arrangement of the carbon atoms, the cylinders are semiconducting or metallic conductors. The tubes can be closed or open at one end or both ends.

Furthermore, when compared with other film field emitters such as diamond or amorphous carbon structures, CNTs show a high aspect ratio, a small radius of curvature of the cap and good conductance (Rinzler *et al*. 1995). Moreover, CNTs have both an extremely large Young modulus and maximal tensile strength. CNTs are chemically highly inert, and react only under extreme conditions or at high temperature with oxygen or hydrogen (Saito *et al*. 1998). Besides, carbon has one of the lowest sputter coefficients (Paulmier *et al*. 2001), which is an advantage as an electron source is usually bombarded by positive ions.

In this review we will try to give an overview of the present status of research on CNT field emitters and their applications. First, we will summarize several methods for the realization of field-emission devices with CNTs. In § 3 we will give an overview of the electron emission properties and in § 4 several examples will be given of devices with CNT electron emitters.

2. Realization of field-emission devices from CNTs

Carbon nanotubes can be used as electron sources in two different types of set-up, namely in single- and in multiple-electron-beam devices. One possible application of a single-electron-beam instrument is an electron microscope that uses a single nanotube as a field-emission electron gun to produce a highly coherent electron beam. Conversely, flat-panel displays are the most popular example of multiple-beam instruments where a continuous or patterned film of nanotubes provides a large number of independent electron beams.

There are two basic types of techniques used for CNT synthesis, namely the vaporization methods (arc discharge, laser) and the catalytic decomposition of hydrocarbons over metal catalysts (also termed CVD methods, for chemical vapour deposition). Basically, three methods exist for building field-emission devices from nanotubes. Nanotubes can be mounted by means of nanomanipulation, devices can be made from 'bulk' samples of nanotubes and nanotubes can be grown directly on desired positions. The three methods are outlined below.

(*a*) *Mounting single CNTs*

It is relatively simple to make a field emitter with CNTs by mounting them on a metal support tip using micromanipulators and an optical microscope (Rinzler *et al*. 1995). Electron emission can be obtained by applying a voltage difference of a few hundred volts to a thousand volts between the support and a counter electrode.

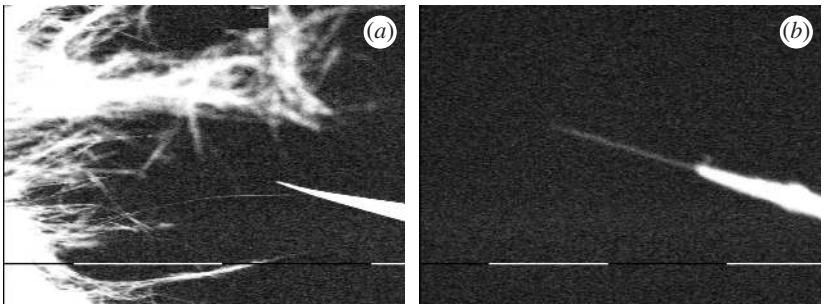

Figure 1. Preparation of a single nanotube electron source (bar represents 10 μm). (*a*) Approach of a CNT sticking out from the main sample by a tungsten tip. (*b*) Nanotube mounted on a tungsten tip after breaking-off the nanotube from the main sample (bar represents 1 μm).

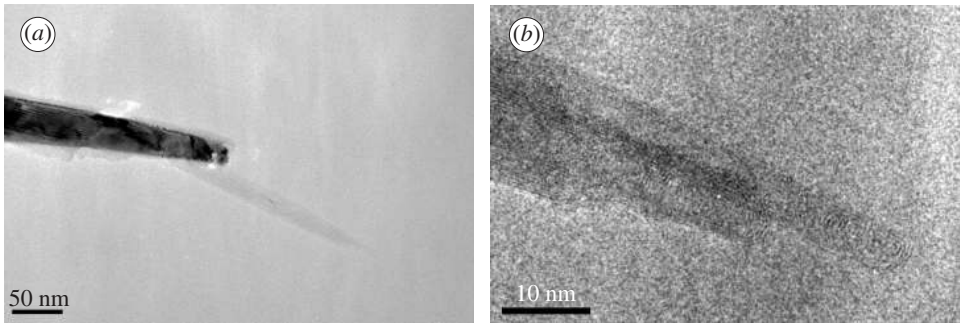

Figure 2. TEM images of an individual multi-walled CNT mounted on a tungsten tip (de Jonge *et al*. 2002). (*a*) The whole nanotube and the end of the tungsten tip can be seen. The glue from the carbon tape, which was used to fix the nanotube, is also visible. (*b*) High-resolution TEM image of the apex of the tube.

To investigate the emission properties of individual CNTs in a more precise way, the mounting method was improved in our laboratory (de Jonge *et al*. 2003) using a piezo-driven nanomanipulator (Omicron NanoTechnology GmbH, Taunusstein, Germany) in a scanning electron microscope (SEM) (Philips Electronics NV, Eindhoven, The Netherlands). For the mounting of an individual CNT on a tungsten tip, a tungsten wire was fixed by laser-welding on a titanium (or tungsten) filament. The end of the wire was etched into a sharp tip (50 nm radius of curvature) using electrochemical etching. In the next step, the tip was transferred into the SEM and carefully pierced into carbon tape. The glue applied on the tip in this manner is necessary for firm attachment of the nanotube. Nanotubes from a batch of arc-discharge grown MWNTs (Colbert *et al*. 1994) were also placed in the SEM and the sample was searched for a long, straight, thin and free-standing nanotube (see figure 1). This nanotube was brought into contact with the tungsten tip, on which it stuck. Finally, the nanotube was broken off the nanotube sample by applying a mechanical force. Alternatively, breaking can occur by Joule heating with a current of more than 20 μA (corresponding to a current density higher than 6×10^{10} A m^{-2} for a tube with a radius of 10 nm!).

The length and the diameter can be selected with this method to a precision of 200 nm and 10 nm, respectively. One would think that only open nanotubes would be obtained after the breaking, but closed nanotubes were observed as well. As can

be seen in figure 2, an individual CNT of a length of only 200 nm and with a closed cap was mounted on a tungsten tip. The surprising observation that the cap was closed after breaking-off the nanotube can possibly be explained in two different ways. Either the nanotube was closed within a bundle that broke at the cap of the nanotube that was connected to the tungsten tip, or the nanotube broke with an open end. In the latter case, the cap was formed through the applied current (and related heating) during the break-off or during the subsequent emission test. The possible existence of an auto-closing mechanism was also discussed by others (Dean & Chalamala 2003).

A slightly different method was used by others to mount nanotubes on scanning probe tips (Nishijima *et al.* 1999), where the nanotube was fixed by growing a contamination layer with the electron beam of an SEM (Nakayama *et al.* 2000). The nanotubes can even be shortened in a controlled manner using electron emission (Akita & Nakayama 2002). Others have picked-up individual CNTs from a surface using an atomic force microscope (Hafner *et al.* 2001).

(*b*) *Realization of CNT films*

A second approach is to realize films either by pressing nanotube powder or spraying a nanotube-containing suspension on a support. The nanotubes can be fixed tightly using carbon glue or paste. A slightly different way is to disperse the nanotubes in an epoxy matrix (Choi *et al.* 1999) and to apply the resulting paste to a substrate. These methods can also be used to obtain a film of nanotubes on a tungsten filament. Their main advantages are that they are simple, that high-quality arc-discharge or laser vaporization nanotube samples can be used, and that the resulting cathodes have in general low turn-on voltages for electron emission. In fact, most devices that have been demonstrated up to now have been realized with such post-growth techniques (Choi *et al.* 1999; Saito & Uemura 2000; Wang *et al.* 2001; Yue *et al.* 2002).

These techniques also permit the realization of patterned films; patterning is essential for devices such as flat-panel displays, where pixels have to be defined. In that case, the nanotube/epoxy paste is pressed into channels etched in a glass substrate, and the surface of the cathode is polished after curing the epoxy to expose the microchannels (Wang *et al.* 1998). It seems in any case that an activation step (for example, by plasma etching (Chung *et al.* 2000)) is necessary to obtain field emission.

Even though post-growth techniques are simple and yield apparently good results, it turns out that the field emission is often dominated by a few nanotubes, and that as a result, the emission site density is very low. This is a drawback for display applications and underlines the need for a better control of the morphology of the nanotube films. On an ideal field-emission cathode, all emitters should have exactly the same dimensions (spacing, length and diameter) to have an uniform field amplification. We outline in the next section how CVD methods allow the control (at least in part) of this morphology.

As a result of the domination of only a few nanotubes in the field emission, experiments on individual nanotubes could be carried out without having to grow or mount a single nanotube. However, the relation between the morphology and the emission properties cannot be properly investigated, as the emitting nanotube most likely differs from the average nanotubes (Bonard *et al.* 2002*b*).

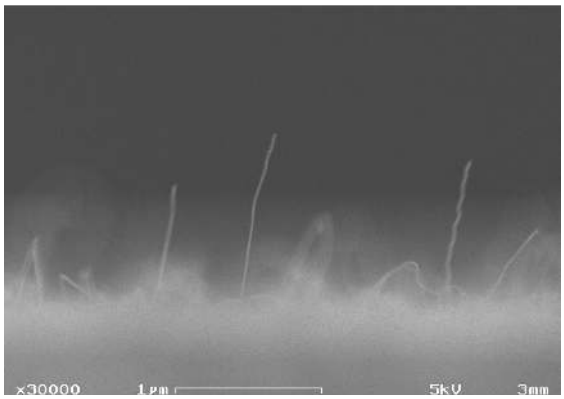

Figure 3. SEM image of a sparse CNT film grown by CVD.

(*c*) *Direct growth of CNTs*

A third way to construct a field-emission device with CNTs is by direct growth on a support structure using CVD techniques. In that case, the carbon source is a hydrocarbon gas. The growth has to be catalysed by a metallic catalyst, such as Fe or Ni. Figure 3 shows an example of a film grow by hot-filament CVD over an Fe-containing catalyst to produce a surface with well-separated nanotubes. One advantage of CVD techniques is that the nanotubes grow only where the catalyst is present on the surface. This means in turn that patterned nanotube films can be grown if a catalyst pattern is defined on the substrate, e.g. by photo- or e-beam lithography (Ren *et al*. 1999; Teo *et al*. 2003), shadow masking or soft lithography (Bonard *et al*. 2001*b*). The second advantage is that the morphology of the film can be controlled to a great extent.

The density of the nanotubes can be adjusted with the amount of catalyst delivered on the substrate from very sparse nanotubes to dense walls (Bonard *et al*. 2001*b*). This density adjustment has proven to be extremely important for tuning the emission properties (emission fields and emission-site densities) of nanotube films (Bonard *et al*. 2001*b*).

The diameter of the nanotubes depends directly on the diameter of the catalyst particle that seeds the growth. This diameter can be controlled in several ways, e.g. by dispersing particles of well-defined size (such as ferritin particles) into an inert matrix (such as Al) (Bonard *et al*. 2002*a*). Finally, it seems from some experiments that the length of the nanotubes may be controlled, provided that there is H_2 present in the reaction atmosphere. An example is shown in figure 4, where an array of 100 nm large Ni dots was used to grow a matrix of aligned individual nanotubes of uniform radius and length (Ren *et al*. 1999; Teo *et al*. 2003). For 100 nm Ni dots, the tip diameter was 49 ± 2 nm and the length was 5.9 ± 0.4 μm. It was also found, using a scanning micro-tip to measure the emission from individual tubes (Semet *et al*. 2002), that the electron emission of neighbouring nanotubes occurred at similar voltages (Teo *et al*. 2003). The CVD technique is hence highly promising, as it presents a controlled process for the production of emitter devices. The main disadvantage is that the nanotubes produced with this method are not of such high quality as arc-discharge or laser-vaporization grown nanotubes (figure 5).

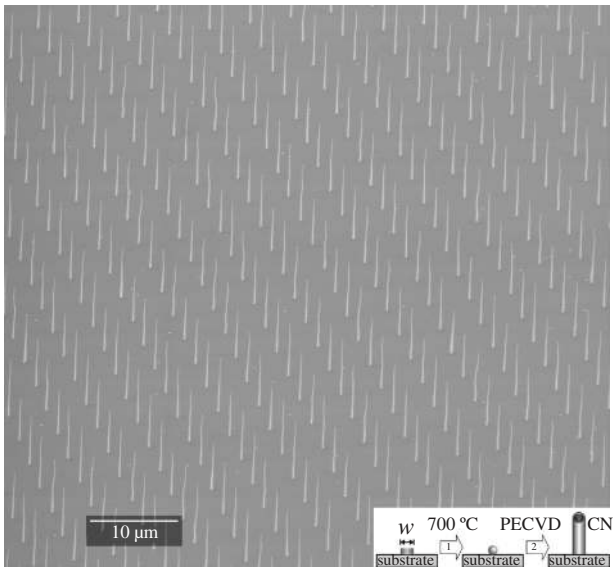

Figure 4. CNTs grown on a support at precisely defined positions using plasma-enhanced CVD. (Reproduced with permission from Teo *et al.* (2003).) The nanotubes were grown from 100 nm wide dots of 7 nm thick Ni catalyst.

As CVD growth occurs only where a catalyst is present, the incorporation of nanotubes into gated structures is also readily possible (Guillorn *et al.* 2001; Lee *et al.* 2001; Leopold *et al.* 2001; Pirio *et al.* 2002). These structures allow a pixel-by-pixel control of the emission of the nanotubes with small voltage differences (typically a few tens of volts) and allow expansion to large matrices of emitters. Finally, nanotubes can be directly grown by CVD on support tips instead of being mounted. Nanotubes grown on Si pyramids have thus been used as imaging probes for atomic force microscopy (Yenilmez *et al.* 2002). The direct growth on a tip is also enhanced by an electric field (Campbell *et al.* 2002; Thong *et al.* 2002).

3. Electron emission from CNTs

(*a*) *Field emission*

A CNT emits electrons under the influence of a large electric field at the cap (figure 6). Its performance can be predicted theoretically if one assumes that the nanotube behaves as a sharp tip showing metallic behaviour: in this case, the emission mechanism will be field emission. The Fowler–Nordheim theory (Fowler & Nordheim 1928; Gadzuk & Plummer 1973; Good & Mueller 1956) describes the field-emission process in terms of a tunnelling current through a potential barrier between a metal surface and vacuum. The current density J is described by (Hawkes & Kasper 1996)

$$J = \frac{e^3F^2}{8\pi h\phi t^2(y)} \exp\left\{ -\frac{8\pi\sqrt{2m}\phi^{3/2}}{3heF} v(y) \right\}, \tag{3.1}$$

$$y = \frac{1}{\phi}\sqrt{\frac{e^3F}{4\pi\varepsilon_0}}, \tag{3.2}$$

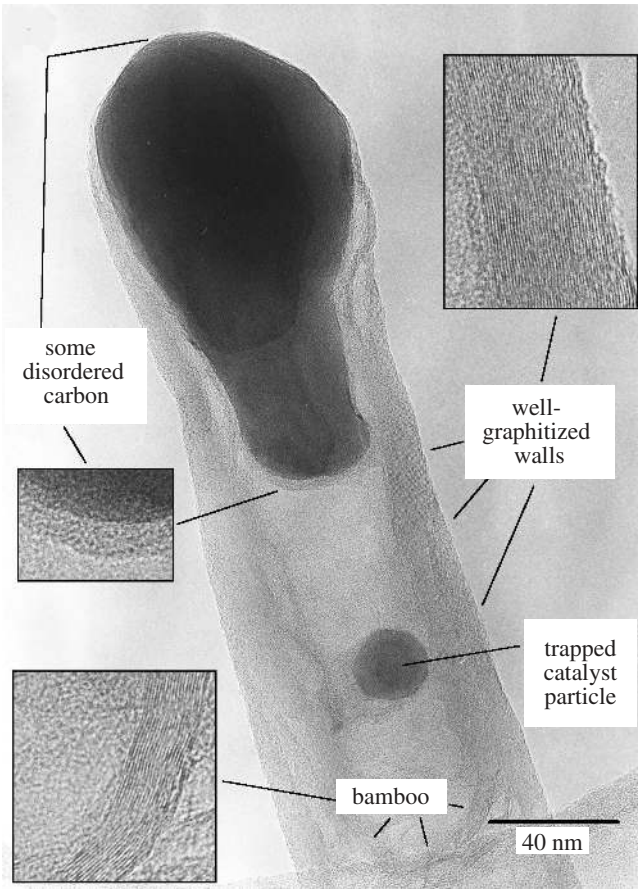

Figure 5. TEM image of a nanotube grown with plasma enhanced CVD. (Reproduced with permission from Teo *et al*. (2003).) The graphite walls and the catalytic particle are visible at the top, and the graphitic structure shows many disruptions.

with workfunction ϕ, electron mass m, electric field F, Planck's constant h, electron charge e, permittivity of free space ε_0 and the functions $t(y)$ and $v(y)$. The functions $t(y)$ and $v(y)$ can be approximated by (Hawkes & Kasper 1996) $t(y) = 1 + 0.1107y^{1.33}$ and $v(y) = 1 - y^{1.69}$. For the case of a triangular surface potential barrier, such that $t(y)$ and $v(y)$ are unity, the function can be approximated by

$$J = 1.54 \times 10^{-6} \frac{F^2}{\phi/e} \exp\left\{ -6.83 \times 10^9 \frac{(\phi/e)^{3/2}}{F} \right\}. \tag{3.3}$$

Here the quantity ϕ/e is the workfunction in electronvolts, which is commonly used. The model is strictly valid only for emission from flat surfaces at 0 K but has proven to be adapted well to describe field emission from sharp tips up to temperatures of several hundred degrees Celsius (Good & Mueller 1956). Corrections of this model are required for tips with extremely curved surfaces (Edgcombe & Johansen 2003; Edgcombe & Valdre 2000). Note also that two other emission mechanisms play a role at higher temperatures (above 1000 K): namely, Schottky emission and thermionic emission. An additional correction may furthermore be necessary in the case of nano-

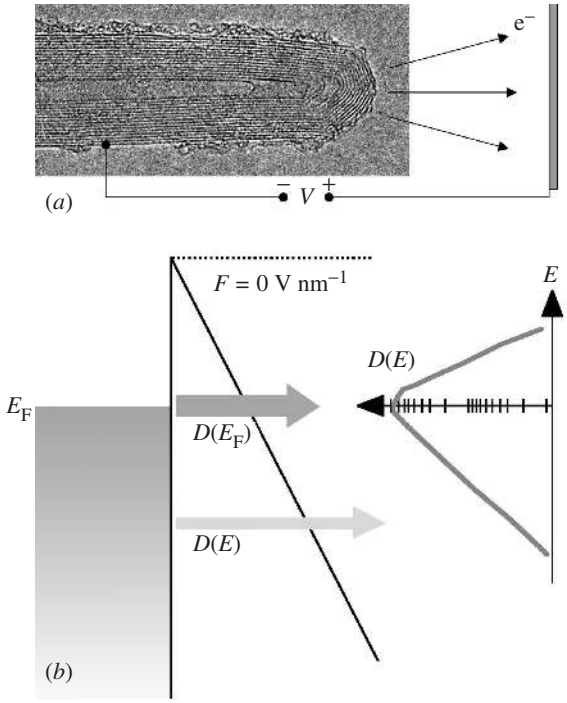

Figure 6. (*a*) Schematic of a field-emission experiment: a potential is applied between a nanotube (TEM micrograph) and a counter electrode. (*b*) Standard field-emission model from a metallic emitter, with the transmission probability as a function of energy $D(E)$.

tubes since the density of states is not energy independent around the Fermi level as in 'real' metals (Saito *et al*. 1998). Yet it was found experimentally that the emission of several types of CNTs could be described to first approximation by the simple model of field emission and a workfunction of 5 eV (Groening *et al*. 2000) (see figure 7). A work function of 4.6–4.8 eV was also found, using a local Kelvin Probe method (Gao *et al*. 2001). Due to the exponential behaviour, the emitted current will be very sensitive to the small variations of the workfunction that can occur between different electronic structures of a material, or that can be induced by adsorbed species.

(*b*) *Field-enhancement factor*

The high electric field required for field emission is obtained close to surfaces of strong curvature, such as the sharp tip of a finely etched wire. At the surface of a free sphere of radius r the field at a potential U is given by

$$F = \frac{U}{r}. \tag{3.4}$$

At the surface of a tip, the field is reduced from this value by the presence of the tip shank, which is taken into account by an empirical correction factor k so that:

$$F = \frac{U}{kr}. \tag{3.5}$$

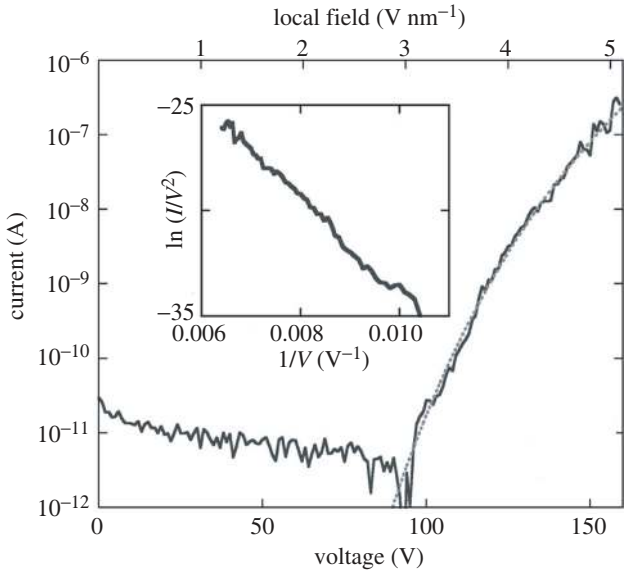

Figure 7. I–V characteristic (————) and corresponding Fowler–Nordheim plot (− − − −) of an individual CNT (the SEM image is given in figure 10). The emission follows the Fowler–Nordheim model over many orders of magnitude of the emitted current, which allows the field-enhancement factor to be estimated to $\gamma \approx 90$ by taking $\phi \approx 5$ eV. (See Bonard *et al*. (2002*b*) for details.)

k is taken usually as $k \approx 5$ for a hemisphere on a cylinder (Dyke & Dolan 1956; Gomer 1961). In a more realistic picture, the field strength also depends on the extractor distance and the shape of the tip. One can use instead the model of Dyke & Dolan that takes into account the geometry of both emitter and experimental set-up (Dyke & Dolan 1956), or rely on numerical simulations to estimate the dependence of the field strength on the extractor distance and the shape of the tip.

Different equations are generally used when the emitters are supported on a flat surface instead of on a tip (Forbes *et al*. 2003):

$$F = \gamma \frac{U}{d}, \tag{3.6}$$

where d is the distance between the extractor and the substrate surface and γ is the field-enhancement factor. An expression for the field-enhancement factor as function of the height of the nanotube h and its radius r was derived by Edgcombe & Valdre (2000):

$$\gamma = 1.2\left(2.15 + \frac{h}{R}\right)^{0.90}, \tag{3.7}$$

with the height of the nanotube h and the base radius R. Equation (3.6) does not make any predictions as to the influence of the counter electrode, and especially of the inter-electrode distance d, although experimental results show that γ varies with d (Bonard *et al*. 2002*b*).

These models apply to a hemisphere on a cylinder, which corresponds to a nanotube with a smooth and clean hemispherical cap. In real-life situations, however, this condition is often not met. The tip of nanotube emitters (especially for MWNTs)

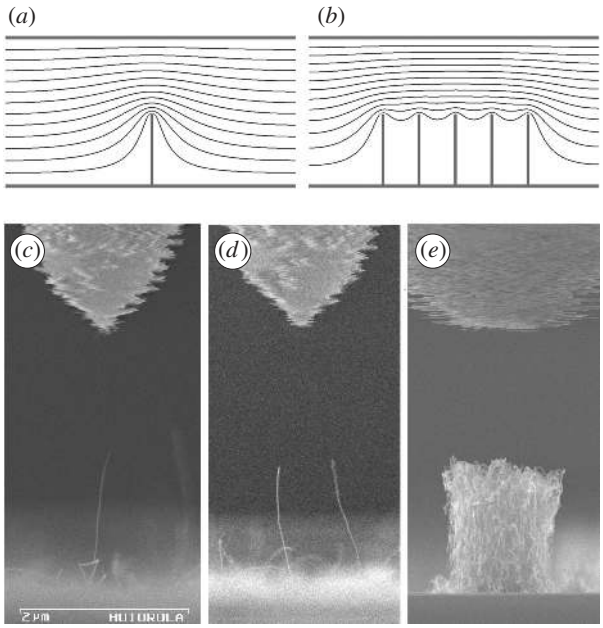

Figure 8. Simulation of the equipotential lines of the electrostatic field for (*a*) a single nanotube on a surface and (*b*) for an assembly of five nanotubes. The field-enhancement factor is lower by a factor of two for the latter case. (*c*)–(*e*) SEM images of three experimental situations. Emission onset was observed at 90 V for (*c*), while no emission was observed up to at least 200 V for (*d*) and (*e*).

is seldom hemispherical but tapered, and may furthermore be flat, opened and/or present nanometre-sized protrusions. Numerical simulations reveal that a deviation from the hemispherical shape produces an increase in the field-enhancement factor up to a factor of two, which can easily lead to a factor of 10 difference in the emitted current. Irregularities on an atomic level of the tube end are not expected to influence the emission properties for a metallic cap, as the electron cloud smooths out these irregularities as in metals (Gomer 1961).

Another important effect comes into play as soon as several emitters are assembled to form an array, namely electrostatic screening between the emitters. Several studies, both theoretical and experimental, reveal that the electric field at the apex of the emitters decreases with decreasing spacing x. In fact, the effective field amplification drops rapidly for a spacing $x = 2h$. This effect influences critically the field-emission properties of individual nanotubes and of nanotube films (Bonard *et al*. 2001*b*; Nilsson *et al*. 2000). As shown in figure 8, the field enhancement is largest for a single nanotube and decreases as soon as nanotubes are positioned close by (Groening *et al*. 2000; Nilsson *et al*. 2000). A field-emission device often requires a high current density. Due to this shielding effect, the configuration yielding the largest current density will often not be the situation with the highest density of nanotubes, but the configuration with an optimum between the largest distance between the tubes on the one hand and the highest density on the other hand.

The fact that the emitted current varies in an exponential way with the electric field, while the field strength is influenced by many factors, is the main drawback

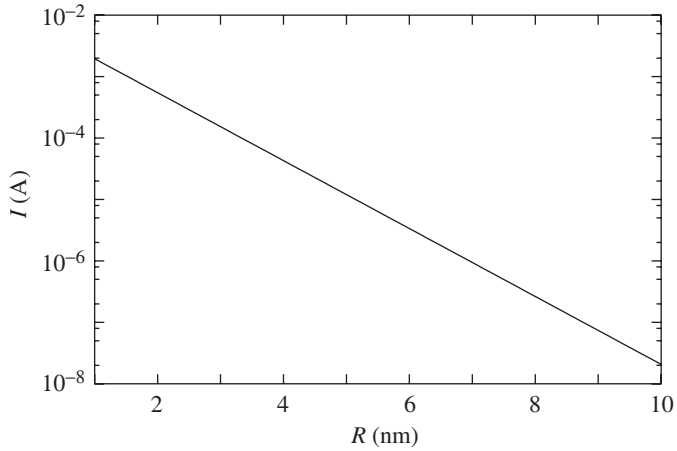

Figure 9. Emitted current of a CNT as function of its radius. The current was calculated with the Fowler–Nordheim theory, for a workfunction of 5 eV, $U = 300$ V and $k = 5$.

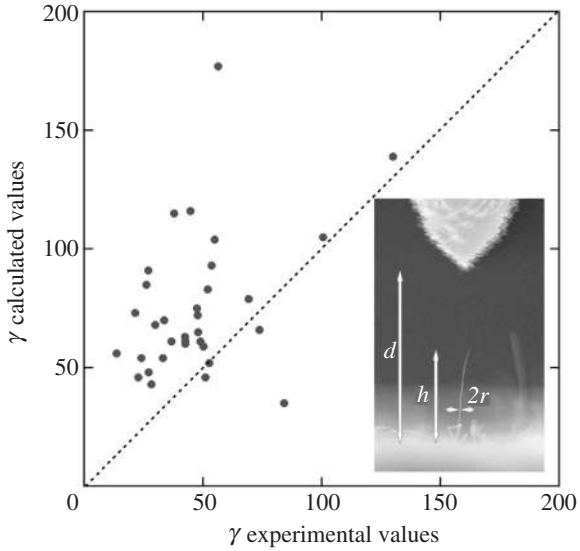

Figure 10. Comparison between the field-enhancement factor determined from the Fowler & Nordheim plot (experimental values) and that estimated from the emitter dimensions as measured by SEM (see inset) for 40 emitters. (See also Bonard *et al.* (2002*b*).)

of CNT electron sources (and of field emitters in general). Even a small variation in the field produces a huge difference in the emitted current. This is demonstrated in figure 9: the emitted current predicted by the Fowler–Nordheim model varies over many orders of magnitude for variations of only a factor of 10 in the radius of the nanotube cap. Another example of the large variations that can be obtained is shown in figure 10, where the field-enhancement factors obtained from measurements of 40 individual nanotubes in an SEM are compared with the values predicted from the measured parameters h, r and d. The two values differ significantly: in fact, the agreement is within the experimental error for only 30% of the measurements

(Bonard *et al.* 2002*b*). We believe that these results show that the emission process is highly sensitive to the exact structure of the cap.

The exponential behaviour of field emission has a second important consequence. Many field-emission devices require both a high current density and a high density of emitting sites. Ideally, a large number of nanotubes should emit a relatively small and similar current, so that their lifetime will be long and the current fluctuations of many nanotubes are averaged-out. These current fluctuations are related to emission of nanotubes that are not sufficiently cleaned and that are not operated in ultra-high vacuum, e.g. in low cost applications. In practice, however, one finds that a single or a few nanotubes provide the emitted current for a pixel area: a nanotube needs to be only slightly thinner, longer or sharper than the surrounding nanotubes to dominate the emission. This effect can even be increased when nanotubes have an open cap or an adsorbed species on the cap.

This effect has been investigated by comparing the measurements on a nanotube film over a large area (average behaviour of *ca.* 1000 emitters cm^{-2}) and on individual emitters from the same film. This experiment showed that the field enhancements are far higher in the former case than in the latter (Bonard *et al.* 2002*b*). The field-enhancement factor determined from the large area measurements represented actually only a very small population of the nanotubes. This effect is critical for most devices, where a homogeneous emission and high emission site density is needed. In fact, the dispersion on γ (and hence on the combination of nanotube height, length and spacing) should be less than 4%, which is difficult to achieve even when the growth is well controlled (Semet *et al.* 2002). One possibility to circumvent this problem may be to include a suitably scaled ballast resistor in series with the emitter to produce a voltage drop above a given current.

(*c*) *Shape of the emitted electron beam*

The electron beam that is emitted from a nanotube is not uniform, but shows certain patterns when projected on a screen, depending on the type of cap. A CNT with an open cap produced a hollow electron beam in some experiments (Hata *et al.* 2001; Saito *et al.* 1997), but we have found other patterns as well.

Emission patterns with a clearly visible symmetry were observed for MWNTs (Saito *et al.* 2000). Figure 11 shows an experiment where a MWNT is heated at 1300 K. The emission pattern contained rings with fivefold symmetry and certain bright spots that disappear in time. The behaviour is typical of absorbed species on the cap. The emitted current decreased as each molecule (bright spot) was removed. The current emitted by the clean tube was lower by a factor of three than the 'dirty' tube: this shows that, on CNTs, adsorbed species enhance the field emission (Dean & Chalamala 2000; Hata *et al.* 2001). The origin of the fivefold symmetry was explained by the structure of the carbon atoms at the cap, consisting of both five- and sixfold carbon rings.

Different patterns were observed with samples containing single-walled nanotubes (SWNTs) and thin MWNTs. A fresh sample usually produced one or more bright spots (lobed patterns) that vanished by heating to about 900 K, after which a pattern with some fine structure was visible (Dean & Chalamala 1999*a*). Sometimes, patterns

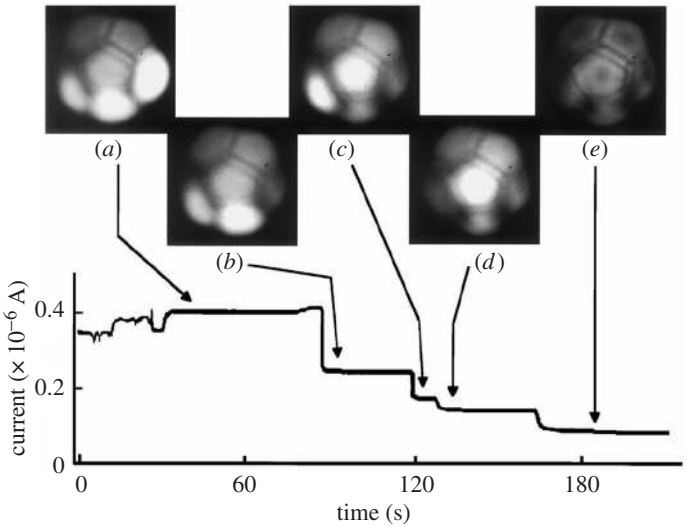

Figure 11. Emission pattern of a multi-walled CNT heated at 1300 K at several points in time (Hata *et al*. 2001). The emitted current as function of time is also shown.

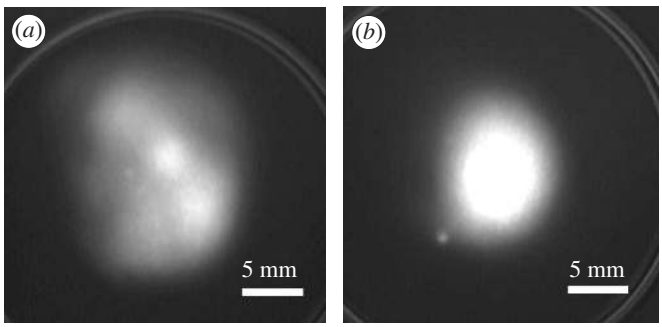

Figure 12. Emission pattern of a multi-walled CNT recorded with a phosphor screen and a microchannel plate (de Jonge 2004). The emitter was positioned *ca*. 2 cm below the microchannel plate. (*a*) Pattern after heating at 1000 K for 10 min, operated at 800 K and a total current of 500 nA. (*b*) Temporal emission pattern of the nanotube for the case of insufficient heating.

with a bright spot in the middle were found and these patterns even started to rotate when the applied electric field was above a certain threshold value (Dean & Chalamala 2003). We observed similar patterns for samples made of individual multi-walled CNTs mounted on tungsten tips (de Jonge 2004) (see figure 12).

We expect that nanotubes with a closed cap with high symmetry, for example, a purely hemispherical cap, will result in a pattern with a clearly visible symmetry. The symmetry of the pattern is disturbed when the cap does not have a perfect shape, but is for example flattened as in figure 2. The bright spots are usually explained by the existence of adsorbed species, but it should also be noted that the cap may contain small protrusions (Kuzumaki *et al*. 2001). Open caps should produce irregular and changing patterns, due to their sharp edges and dangling bonds. Irregular patterns were also observed for damaged caps, consisting of amorphous carbon.

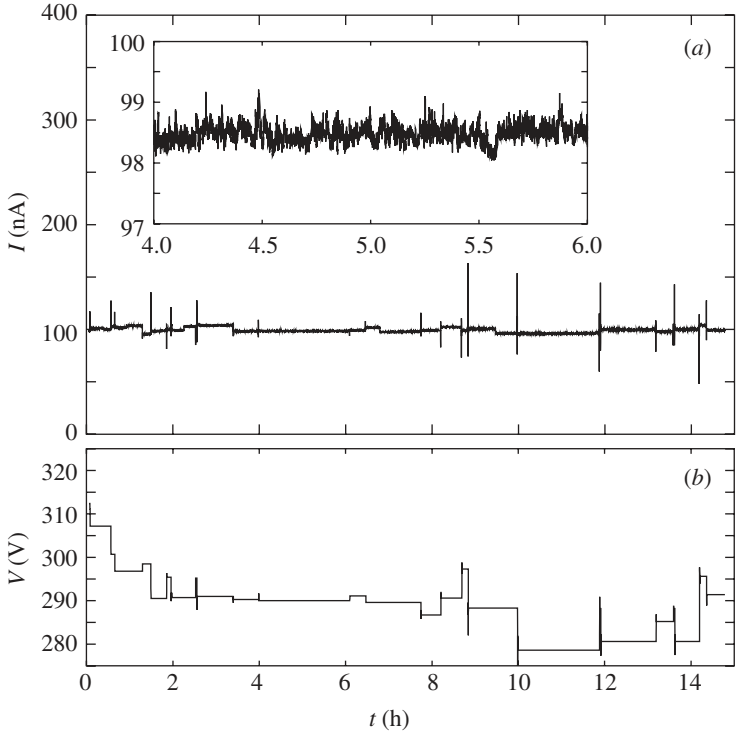

Figure 13. (*a*) Emission current with active current regulation measured every second and (*b*) corresponding extraction voltage of a CNT electron source as a function of time (de Jonge & van Druten 2003). The inset shows in detail a period of stable emission in which the current fluctuated less than 1%, at constant extraction voltage over more than 2 h.

(*d*) *Emission stability*

Field emission from an emitter at room temperature is inevitably associated with fluctuations of the emitted current over time (Hainfeld 1977). This is caused by the exponential behaviour of field emission with the applied field and the workfunction as discussed above. Small molecules absorbed on the cap may lead to slight changes in the workfunction or of the cap geometry, resulting in large differences in the emitted current. Even in ultra-high vacuum the absorption of molecules from the vacuum cannot be prevented and molecules may reach the cap by surface diffusion. Moreover, the structure and electronic structure of the emitter itself may change slightly. The potential benefit of the CNT electron emitter becomes clear considering that it has a structure of carbon atoms bound by covalent bonds. As a result, the nanotube emitter may suffer little from surface diffusion of the emitter material in the presence of the large electric field required for field emission. This enables the use of the CNT as an extremely small point source of electrons, while operating it at stable currents up to microamperes. Moreover, the CNT has an extremely large Young modulus, is chemically highly inert and is sputter resistant (Saito *et al*. 1998).

There are several ways to reduce the current fluctuations. Of critical importance is the initial cleaning of the CNT, as a new nanotube can easily show fluctuations of over a factor of four. Usually, the emitter is heated to a temperature of *ca.* 1000 K

in ultra-high vacuum (Dean & Chalamala 1999*a*) to remove adsorbed molecules or impurities (de Jonge & van Druten 2003; Saito *et al*. 1998; Yaguchi *et al*. 2001). Others stabilized the emission by setting an emission current of over 1 μA for several minutes, which was explained by self-heating of the nanotube (Purcell *et al*. 2002*a*). The latter method requires nanotubes that are sufficiently long and have a good electrical contact with the support. When the nanotube is cooled down to room temperature after the initial heating, some fluctuations remain and once every while a large current jump takes place. The current fluctuations can be kept small by an active current regulation, as shown in figure 13. It is also of advantage to use a series resistor of several MΩ (ballast resistor). An important question is how stable the average electric field around the cap is in time. It was found by electron holography experiments that the electric field remained remarkably constant, although large fluctuations of the emitted current did take place (Cumings *et al*. 2002).

The stability can be largely increased when the temperature is kept at 600–900 K, so that absorbed molecules are continuously driven off the nanotube (de Jonge 2004). When the emitter fulfils the requirement for self-heating, it may also be possible to obtain stable emission without additional (external) heating (Purcell *et al*. 2002*a*). A clean nanotube is sensitive to molecules in the vacuum, and especially to oxygen, which can cause irreversible damage to the tube. Noble gases usually cause an increase in the current fluctuations, but the emission stability is restored after evacuation of the gas (Dean & Chalamala 1999*b*). The vacuum level should be of the order of 10^{-9}–10^{-10} mbar for emission stability of a few per cent, but lower vacuum levels are also allowed at the cost of stability. For lower vacuum levels it would be of advantage to reduce the partial pressure of oxygen and water.

(*e*) *Lifetime and failure mechanisms*

The lifetime of an individual CNT electron source is long, many hundreds of hours (Dean & Chalamala 1999*b*; Fransen *et al*. 1999). The latest lifetime test in our lab has already shown continuous operation of four CNT sources over 16 months at a current of 100 nA, a vacuum level of 2×10^{-10} mbar and at a temperature of about 800 K. The experiment is still running and none of the emitters shows any damage.

Nevertheless, the failure of nanotube emitters is witnessed for single emitters as well as for emitter arrays. The phenomena leading to the degradation of the emitters are not completely understood at present, and it seems that several factors play a role. Firstly, electrostatic deflection or mechanical stresses can cause alterations in the shape and/or surroundings of the emitter, which may lead to a decrease in the local field amplification.

Secondly, high currents can rapidly damage a nanotube. A gradual decrease in field enhancement due to field evaporation was found on SWNTs when the emitted current was increased beyond a given limit (300 nA–1 μA) (Dean *et al*. 2001). On MWNTs, a shortening of the emitter over time (Wei *et al*. 2001) or damage to the outer walls of the nanotube due to high currents (Wang *et al*. 2002) were also reported. Tube layers or caps are removed, peeled back, or the end of the tube is amorphized (Wang *et al*. 2000, 2002). Typically, MWNTs can be operated at currents of up to 10 μA, but the current should be kept below 1 μA for stable operation and long life-time (de Jonge 2004). In all cases a strong decrease in the emission current occurs and the voltage has to be substantially increased to obtain comparable currents.

Thirdly, it seems that residual gases have a significant influence. Irreversible damage can occur through bombardment from gas molecules ionized by the emitted electrons (Dean & Chalamala 1999*b*). Especially, exposure to oxygen, or water may lead to irreversible decreases in the current, while the nanotube is less damageable by exposure to Ar and H_2 (Dean & Chalamala 1999*b*).

The above mechanisms involve a gradual degradation of the emitters, but the failure can also be abrupt. On multi-walled CNTs grown by CVD, abrupt failures occurred during field emission in the SEM (Bonard *et al.* 2003). This observation suggests a mechanical failure mechanism due to the tensile loading of the emitter under the applied electric field and/or to resistive heating at the contact. The former mechanism could be assigned to failures occurring at applied fields and currents below $4\ \mathrm{V\ nm^{-1}}$ and $1\ \mu\mathrm{A}$, respectively, and the latter to failures occurring at higher fields and currents.

Another catastrophic mechanism is arcing, i.e. an arc between cathode and anode that is initiated by field emission. Such arcing events are commonly observed on diamond and diamond-like carbon films (Groening *et al.* 1996). They are usually caused by a high field-emission current, anode out-gassing, or local evaporation of cathode material that creates a conducting channel between the electrodes.

(*f*) *Energy spread*

For applications of the electron source in which the electron beam has to be focused into a fine spot, such as electron microscopes and electron-beam-lithography machines, the energy spread of the emitted electron beam is of high importance. A large energy spread leads to chromatic aberrations of the electron optical system, reducing the resolution of the instrument. The expected energy spread can be calculated by expressing the current density as function of the energy using the Fowler–Nordheim theory (Hawkes & Kasper 1996):

$$J(E) = \frac{4\pi med}{h^3} \exp\left\{ -\left(E - \frac{2v(y)}{3t(y)}\phi\right)\frac{1}{d}\right\}\left(1 + \exp\left(\frac{E}{k_{\mathrm{B}}T}\right)\right)^{-1}. \tag{3.8}$$

Here, k_{B} is the Boltzmann constant, T is the temperature and the tunnelling parameter d is given by

$$d = \frac{ehF}{4\pi\sqrt{2m\phi}t(y)}. \tag{3.9}$$

The parameter d can be expressed for $t = 1$ as

$$d = 9.76 \times 10^{-11}\frac{eF}{(\phi/e)^{1/2}}. \tag{3.10}$$

The energy spread of the source ΔE is defined by the full width at half maximum (FWHM) of the energy spectrum and is determined by d and T.

Several experiments revealed a small energy spread of 0.2–0.3 eV as expected for a cold field emitter and only small deviations from the Fowler–Nordheim theory (Bonard *et al.* 1999; de Jonge & van Druten 2003; Groening *et al.* 2000), for both single-walled CNTs and several types of multi-walled CNTs (see, for example, figure 14). Recent experiments showed that the energy spread increased mildly with increasing temperature, as expected from the Fowler–Nordheim theory, and did not

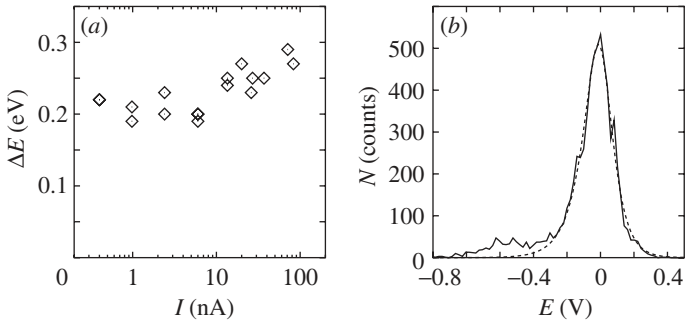

Figure 14. Measurements of the energy spectrum of an individual CNT mounted on a tungsten tip (de Jonge & van Druten 2003). (*a*) The energy spread as function of the emitted current. (*b*) The energy spectrum at 2.4 nA with an FWHM of 0.20 eV. The dashed line indicates the fit with the Fowler–Nordheim theory.

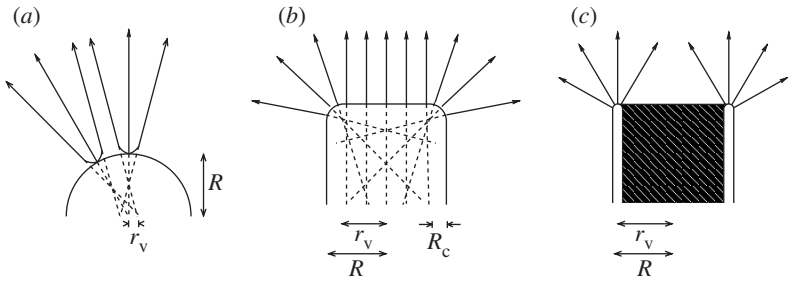

Figure 15. Models of the virtual source (de Jonge 2004). (*a*) Electron trajectories as emitted from a spherical cap of a field emitter with radius R. The back-traced trajectories cross in a surface with radius r_v. (*b*) Electron trajectories as emitted from a nanotube with a flat cap. The back-traced trajectories cross in a surface with radius r_v, slightly smaller than the radius of the tube R. The radius of curvature at the edge of the cap is R_c. (*c*) Nanotube with an open cap.

deviate significantly from this mechanism for temperatures up to 900 K. Yet the model may not apply to the CNT in all cases and a refined model may be necessary (Filip *et al*. 2001). One report mentioned an energy spread of 0.1 eV, but this value was not reproduced (Fransen *et al*. 1999). In several other experiments, the energy spread turned out to be somewhat larger than predicted by the Fowler–Nordheim theory. Some of our nanotubes had an energy spread of up to 0.5 eV. Data of Hata *et al*. (2001) revealed values between 0.3 and 0.4 eV, and their energy spectra contained a relatively large shoulder at the high-energy side (Takakura *et al*. 2003). These shoulders can probably be explained by self-heating of the nanotube. Indeed, the experiments of Purcell (*et al*. 2002*a*), in which the effect of self-heating was investigated, demonstrated a significant broadening of the high-energy side of the energy spectra as function of the emitted current. Note also that additional features in the emission spectrum above 900 K were observed (Dean *et al*. 1999).

(*g*) *The reduced brightness*

Another important parameter for the resolution in high-resolution electron-beam instruments is the reduced brightness. The reduced brightness B_r measures the amount of current that can be focused into a spot of a certain size and from a

certain solid angle. It is a function of the radius of the virtual source r_v, the angular current density I' corresponding to the brightest fraction of the emitted electron beam and the beam potential U (Hainfeld 1977; Hawkes & Kasper 1996):

$$B_\mathrm{r} = \frac{I'}{\pi r_\mathrm{v}^2 U}. \tag{3.11}$$

The virtual source of an electron emitter is the area from which the electrons appear to originate when their trajectories are traced back (Hainfeld 1977). The virtual source sizes of individual multi-walled CNTs were determined by operating the nanotubes as electron sources in a point-projection microscope (de Jonge *et al.* 2002). It was found that the radius of the virtual source size varied between 2.1 and 3.0 nm for arc-discharge-grown MWNTs (de Jonge 2004). This result was larger than expected for the situation of an emitter with a hemispherical cap and was explained by a flat, or open cap (see figure 15).

The reduced angular current density varied between 19 and 50 $\mathrm{nA\,sr^{-1}\,V^{-1}}$. The angular current density was measured for a cleaned nanotube at the maximal current at which stable emission was obtained (1 μA). The reduced brightness was determined for two emitters and amounted to $(2.5 \pm 1) \times 10^9$ and $(1.3 \pm 0.5) \times 10^9$ $\mathrm{A\,m^{-2}\,sr^{-1}\,V^{-1}\,s}$, respectively. These values are an order of magnitude larger than the values of state-of-the-art commercial sources (Hainfeld 1977; Swanson & Schwind 1997; van Veen *et al.* 2001).

4. Field-emission devices

(*a*) *Field-emission display*

The application area of CNT electron sources with the largest potential market is the flat-panel field-emission display (Choi *et al.* 1999; Saito & Uemura 2000), which provides a high-brightness display for both consumer and professional applications. Figure 16*a* shows the functions of the simplest form of a display pixel. Nanotubes are patterned on a matrix of electrodes in a vacuum housing. The counter electrode is a glass plate coated with a conducting but transparent layer and a phosphor layer. A voltage difference of a few kilovolts between the nanotube cathode and the glass plate results in field emission and the generation of light through excitation of the cathodoluminescent phosphor. An image can be obtained by addressing selectively the different positions of the matrix, which can either be monochrome or in colour if each pixel is divided in red, blue and green sub-pixels.

One may have the impression that a field-emission display is a relatively simple device, but this is not the case. One of the first problems encountered is the occurrence of charging effects at the isolating spacers between the cathode and the anode, so many research efforts have been invested to develop a suitable technology. Another issue is that it is difficult (and expensive) to operate the display with the large voltage difference between the cathode and the anode, which is needed both for extracting electrons and to warrant a sufficient efficiency of the phosphor. One solution is to use a third electrode as a gate (Chung *et al.* 2002) to control the emission with the gate-to-cathode voltage (Choi *et al.* 2003; Jung *et al.* 2002; Yu *et al.* 2002), which enables switching by only a few tens of volts, and to accelerate the electrons to their final energy with a constant gate-to-anode voltage (see figure 16*b*). Moreover,

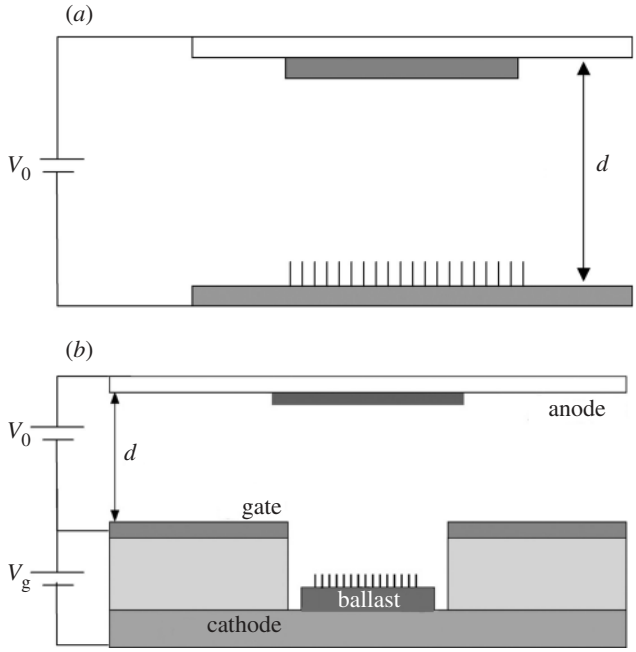

Figure 16. Schematic of the working principle of a field-emission display pixel: (*a*) diode structure; (*b*) triode structure with ballast resistor in series with the emitters.

Figure 17. Prototype of a CNT field-emission display (Chung *et al*. 2002) with a gate structure, an active area of 12.7 cm in diagonal, full colour and 100 Hz.

the gate can be used to converge the electron beam so that higher brightness and a sharper image can be obtained. One emitting pixel should ideally address only one pixel on the screen, but in practice this is often not the case as the electron beam spreads out in space and the direction of the beam varies from nanotube to nanotube. Several prototype displays of this type have been fabricated (Chung *et al.* 2002) (see figure 17).

As discussed in the previous section, a single or a few nanotubes, each emitting currents up to a few tens of microamperes will probably dominate the emission in a pixel area. It is not unlikely that each pixel requires a different gate voltage and must be current regulated individually to obtain stable emission. Furthermore, degradation will take place and lead to the destruction of emitters, so that the emission will be provided by the next longest and thinnest nanotube. The requirements of stability of the emitted current and lifetime could be difficult to meet with structures that incorporate nanotubes directly on the electrodes. One possibility of providing a much longer lifetime per nanotube is to limit the emitted current, e.g. to below a microampere. This can be achieved with a suitably scaled ballast resistor in series with the emitters. This limitation of the emitted current not only protects the emitters against degradation but also significantly improves the homogeneity of the emission, and increases the emission site density to acceptable values. A second option is to construct a display pixel from several sub-pixels, each with a current regulator. Further possibilities are to use nanotubes of a length of a few tens of micrometres so that they can be cleaned by self-heating during the emission, or to employ other types of emitter pixels mentioned in scientific and patent literature. The current of a pixel can also be amplified by a medium such as a microchannel plate (Yu *et al.* 2001), or a hopping electron mechanism (Visser *et al.* 2003).

Field-emission panel displays were demonstrated 10 years ago (Zhu 2001) using Spindt-type emitters (Spindt 1968). The advantages of nanotubes over previously used materials such as silicon or molybdenum are that the technology involved is relatively simple and that the CNT emitter is robust. Human vision is extremely sensitive: when only one pixel on a display does not work, this error is recognized immediately by the human eye and brain. Thus, the lifetime of each pixel should be several years.

(*b*) *Field-emission lamp*

The first device with a CNT cathode to be demonstrated was the field-emission lamp (Chen *et al.* 2003; Saito & Uemura 2000). Such lamps are simple lighting elements where the phosphor layer on the inner surface of the anode is bombarded with energetic electrons emitted by the CNT cathode, as in figure 18, sometimes with the addition of a gate electrode. A first configuration, the so-called 'jumbotron lamp', has the shape of the old vacuum tube, where the top surface is illuminated. It has been under investigation since 1998 and such lamps are available commercially (Saito & Uemura 2000). These tubes form the pixel elements in giant screen displays and have a brightness that is typically a factor of two larger than conventional thermionic lighting elements, with demonstrated lifetimes of 8000 h (Saito & Uemura 2000).

There have been also some attempts to realize lighting elements with field emitters to offer an alternative to incandescent or fluorescent lamps. This can be realized, as in figure 23, with a cylindrical wire on which nanotubes were grown on the cathode,

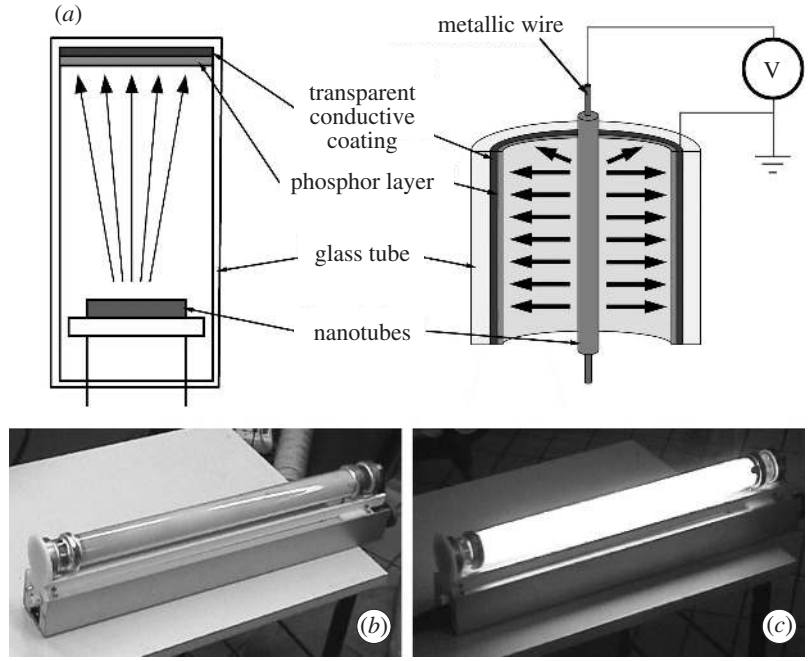

Figure 18. (*a*) Schematic luminescent elements with (left) a flat and (right) a cylindrical luminescent surface. (*b*) and (*c*) Experimental realization of a fully sealed luminescent tube with a CNT cathode. (See also Croci *et al*. (2003).)

placed inside a glass tube with phosphor and conductive layers on the inner surface as the anode (Bonard *et al*. 2001*a*). Fully sealed elements of 40 cm in length were realized: in contrast to usual fluorescent tubes, such tubes contain no mercury, start up instantly, are readily dimmable and can yield higher brightness than the usual fluorescent elements (Croci *et al*. 2003). The luminance reaches that of commercial fluorescent tubes, but the power needed for operation is currently significantly higher than for a fluorescent tube. This difference is mainly due to the efficiency of the phosphor, as cathodoluminescents are approximately five times less efficient than ultra-violet-to-visible phosphors.

(*c*) *X-ray source*

Films with CNTs have also been used in X-ray sources (Sugie *et al*. 2001; Yue *et al*. 2002) and applied in commercial products such as hand-held X-ray spectrometers and mini-X-ray tubes for medical and other applications. A schematic is shown in figure 19. Real X-ray imaging was demonstrated in both continuous and pulsed mode, and a maximal electron emission current of 28 mA was obtained (Yue *et al*. 2002). The vacuum level was 10^{-6}–10^{-7} mbar, which limited the lifetime of the source. The main advantage of the device over conventional X-ray sources is that it does not require a thermionic electron source, which enables miniaturization. Compared with a field-emission X-ray source using a tungsten electron emitter, the benefits are most probably the larger current density, the lower vacuum level and better stability of the emitted current.

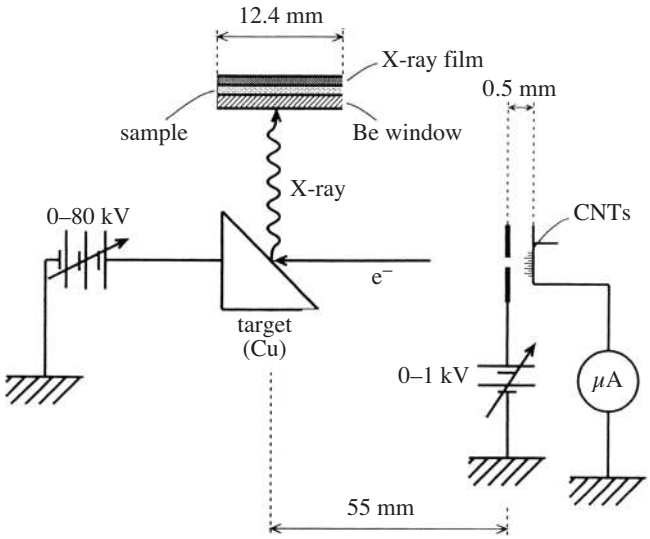

Figure 19. A schematic of the field-emission X-ray tube. (Reproduced with permission from Sugie *et al*. (2001).) A film of CNTs was used as the cathode. The extraction voltage was set by a gate electrode 0.5 mm in front of the nanotube film. The emitted electrons were further accelerated towards a Cu target to produce X-rays.

(*d*) *High-resolution electron-beam instruments*

Electron sources of individual CNTs could potentially improve the resolution and processing speed for certain operation regimes of high-resolution electron-beam instruments, such as electron microscopes, electron-beam-assisted-deposition instruments and electron-beam-lithography instruments. The state-of-the-art source for these instruments, the Schottky emitter (Swanson & Schwind 1997) already produces an electron beam with a high reduced brightness (2×10^8 A m^{-2} sr^{-1} V^{-1} s), a low-energy spread (0.8 eV), a good stability (less than 0.5%) and a long lifetime (years). The commercially available cold field emission has a lower energy spread (0.3 eV) but an inferior stability of the emitted current (*ca.* 5%) (Orloff 1989). In the previous section we have stated that the CNT electron emitter improves on the brightness (de Jonge *et al*. 2002; de Jonge 2004) and energy spread (de Jonge & van Druten 2003) with respect to the Schottky emitter, while maintaining a good emission stability.

Spatial resolution can be enhanced in low-energy SEMs with a reduced energy spread and a higher brightness. Energy resolution can be improved in energy-resolved spectroscopy in the SEM and the transmission electron microscope (TEM) by using an electron source with a lower energy spread (Egerton 2003). A source with a higher brightness has the additional advantage that larger currents can be focused into a given spot size, resulting in shorter image-acquisition times and faster processing times of electron-beam-assisted deposition. It will also be of advantage for systems comprising energy filters (Tiemeijer *et al*. 2001). Finally, the nanotube source is an ideal source for point-projection microscopy (de Jonge *et al*. 2002; Schmid & Fink 1997), avoiding the difficult processing of ultrasharp tungsten sources.

EBL may also benefit from a CNT electron source. Present EBL machines usually have one electron source. A higher brightness could possibly increase the processing

speed of these machines. Another interesting option is to make an array of electron sources with CNTs. An example is to grow individual nanotubes in gate structures and combine these electron sources with micro lenses (Binh *et al*. 1998; Guillorn *et al*. 2001; Leopold *et al*. 2001; Pirio *et al*. 2002).

One of the remaining challenges is the manufacture of CNT electron guns with the desired properties in a reproducible manner, as the knowledge needed to develop a process in which the shape and state of an individual nanotube can be precisely controlled is still lacking. The advantage of the CNT is that the material has many advantageous properties for a high-quality electron source. Furthermore, these professional applications allow a certain amount of processing and do not require extremely cheap sources.

(*e*) *Other applications*

One of the main reasons for the development of field-emitter arrays by Spindt (1968) was to provide a more reliable alternative to the thermoelectronic emitters used in microwave amplifiers (so-called 'travelling-wave tubes') (Jensen 1999). This type of application is very demanding because the current density must be at least 0.1 A cm^{-2} (Jensen 1999). A prototype based on an SWNT cathode is able to reach that lower limit to operate in microwave tubes.

Gas-discharge tubes that serve as an over-voltage protection have also been realized with nanotubes (Rosen *et al*. 2000). When the voltage between a nanotube cathode and a counter electrode reaches a threshold value for field emission, the emitted current induces a discharge in the noble-gas-filled inter-electrode gap. It could be demonstrated that this device shows better performance than commercially available elements.

One particularly elegant idea is the use of an emitting CNT as an electrically driven mechanical resonator, with extremely sharp resonance peaks (Purcell *et al*. 2002*b*). Other examples are space applications, such as the high-precision thrusters needed for the next generation of space telescopes (Marcuccio *et al*. 1997), where seven satellites will have to be positioned with a relative precision of *ca*. 1 nm. Lastly, sensitive gas sensors have been constructed from a film of CNTs (Modi *et al*. 2003; Riley *et al*. 2003).

5. Conclusion

Carbon nanotube electron sources clearly have interesting properties, such as low-voltage operation, good emission stability, long lifetime, high brightness and low-energy spread. Several applications could possibly benefit from the use of CNTs, and considerable research efforts in both academe and industry have been allocated to evaluate these possibilities. The most promising applications are the field-emission display and high-resolution electron-beam instruments. Yet many hurdles remain. First, it is at present difficult to make a single source, or an array of CNT electron sources, with the desired properties in a reproducible manner. Second, it is not easy to make devices with many nanotubes emitting homogeneously in a cost-effective manner. Nonetheless, there has been tremendous progress during the last few years and these hurdles will probably be overcome. Hence, it may well be that a similar

review article in a few years' time will report on reliable and reproducible preparation methods, a better understanding of the emission mechanism, the demonstration of additional original devices, and—why not!—on commercial nanotube electron sources and nanotube field-emission displays.

References

Akita, S. & Nakayama, Y. 2002 Length adjustment of carbon nanotube probe by electron bombardment. *Jpn. J. Appl. Phys.* **41**, 4887–4889.

Binh, V. T., Semet, V., Guillot, D., Legagneux, P. & Pribat, D. 1998 Microguns with 100-V electron beams. *Appl. Phys. Lett.* **73**, 2048–2050.

Bonard, J. M., Salvetat, J. P., Stockli, T., Forro, L. & Chatelain, A. 1999 Field emission from carbon nanotubes: perspectives for applications and clues to the emission mechanism. *Appl. Phys.* A **69**, 245–254.

Bonard, J. M., Stockli, T., Noury, O. & Chatelain, A. 2001*a* Field emission from cylindrical carbon nanotube cathodes: possibilities for luminescent tubes. *Appl. Phys. Lett.* **78**, 2775–2777.

Bonard, J. M., Weiss, N., Kind, H., Stoeckli, T., Forro, L., Kern, K. & Chatelain, A. 2001*b* Tuning the field emission from carbon nanotube films. *Adv. Mater.* **13**, 184–188.

Bonard, J. M., Chauvin, P. & Klinke, C. 2002*a* Monodisperse multiwall carbon nanotubes obtained with ferritin as catalyst. *Nano Lett.* **2**, 665–667.

Bonard, J. M., Dean, K. A., Coll, F. C. & Klinke, C. 2002*b* Field emission of individual carbon nanotubes in the scanning electron microscope. *Phys. Rev. Lett.* **89**, 197602.

Bonard, J. M., Klinke, C., Dean, K. A. & Coll, F. C. 2003 Degradation and failure of carbon nanotube field emitters. *Phys. Rev.* B **67**, 115406.

Campbell, P. B., Snow, E. S. & Novak, J. P. 2002 Simple catalyst for the growth of small-diameter carbon nanotubes. *Appl. Phys. Lett.* **81**, 4586–4588.

Chen, J., Zhou, X., Deng, S. Z. & Xu, N. S. 2003 The application of carbon nanotubes in high-efficiency low power consumption field-emission luminescent tube. *Ultramicroscopy* **95**, 153–156.

Chernozatonskii, L. A., Gulyaev, Y. V., Kosakovskaya, Z. Y., Sinitsyn, N. I., Torgashov, G. V., Zakharchenko, Yu. F., Fedorov, E. A. & Val'chuk, V. P. 1995 Electron field emission from nanofilament carbon films. *Chem. Phys. Lett.* **233**, 63–68.

Choi, W. B. (and 10 others) 1999 Fully sealed, high-brightness carbon-nanotube field-emission display. *Appl. Phys. Lett.* **75**, 3129–3131.

Choi, Y. S. (and 13 others) 2003 A field-emission display with a self-focus cathode electrode. *Appl. Phys. Lett.* **82**, 3565–3567.

Chung, D. S., Choi, W. B., Kang, J. H., Kim, H. Y., Han, I. T., Park, Y. S., Lee, Y. H., Lee, N. S., Jung, J. E. & Kim, J. M. 2000 Field emission from 4.5 in. single-walled and multiwalled carbon nanotube films. *J. Vac. Sci. Technol.* B **18**, 1054–1058.

Chung, D. S. (and 17 others) 2002 Carbon nanotube electron emitters with a gated structure using backside exposure processes. *Appl. Phys. Lett.* **80**, 4045–4047.

Colbert, D. T. (and 11 others) 1994 Growth and sintering of fullerene nanotubes. *Science* **266**, 1218–1222.

Croci, M., Arfaoui, I., Stoeckli, T., Chatelain, A. & Bonard, J. M. 2003 A fully sealed luminescent tube based on carbon nanotube field emission. *Microelectron. J.* **35**, 329–336.

Cumings, J., Zettl, A., McCartney, M. R. & Spence, J. C. H. 2002 Electron holography of field-emitting carbon nanotubes. *Phys. Rev. Lett.* **88**, 056804.

de Heer, W. A., Chatelain, A. & Ugarte, D. 1995 A carbon nanotube field-emission electron source. *Science* **270**, 1179–1180.

de Jonge, N. 2004 The brightness of carbon nanotube electron emitters. *J. Appl. Phys.* **95**, 673–681.

de Jonge, N. & van Druten, N. J. 2003 Field emission from individual multiwalled carbon nanotubes prepared in an electron microscope. *Ultramicroscopy* **95**, 85–91.

de Jonge, N., Lamy, Y., Schoots, K. & Oosterkamp, T. H. 2002 High brightness electron beam from a multi-walled carbon nanotube. *Nature* **420**, 393–395.

de Jonge, N., Lamy, Y. & Kaiser, M. 2003 Controlled mounting of individual multiwalled carbon nanotubes on support tips. *Nano Lett.* **3**, 1621–1624.

Dean, K. A. & Chalamala, B. R. 1999*a* Field emission microscopy of carbon nanotube caps. *J. Appl. Phys.* **85**, 3832–3836.

Dean, K. A. & Chalamala, B. R. 1999*b* The environmental stability of field emission from single-walled carbon nanotubes. *Appl. Phys. Lett.* **75**, 3017–3019.

Dean, K. A. & Chalamala, B. R. 2000 Current saturation mechanisms in carbon nanotube field emitters. *Appl. Phys. Lett.* **76**, 375–377.

Dean, K. A. & Chalamala, B. R. 2003 Experimental studies of the cap structures of single-walled carbon nanotubes. *J. Vac. Sci. Technol.* B **21**, 868–871.

Dean, K. A., Groening, O., Kuttel, O. M. & Schlapbach, L. 1999 Nanotube electronic states observed with thermal field emission electron spectroscopy. *Appl. Phys. Lett.* **75**, 2773–2775.

Dean, K. A., Burgin, T. P. & Chamala, B. R. 2001 Evaporation of carbon nanotubes during electron field emission. *Appl. Phys. Lett.* **79**, 1873–1875.

Dyke, W. P. & Dolan, W. W. 1956 *Advances in electronics and electron physics*, vol. 8, pp. 89–157. Academic.

Edgcombe, C. J. & Johansen, A. M. 2003 Current-voltage characteristics of nonplanar cold field emitters. *J. Vac. Sci. Technol.* B **21**, 1–5.

Edgcombe, C. J. & Valdre, U. 2000 Field emission and electron microscopy. *Microsc. Microanalysis* **6**, 380–387.

Egerton, R. F. 2003 New techniques in energy-loss spectroscopy and energy-filtered imaging. *Micron* **34**, 127–139.

Filip, V., Nicolaescu, D. & Okuyama, F. 2001 Modeling of the electron field emission from carbon nanotubes. *J. Vac. Sci. Technol.* B **19**, 1016–1022.

Forbes, R. G., Edgcombe, C. E. J. & Valdre, U. 2003 Some comments on models for field enhancement. *Ultramicroscopy* **95**, 57–65.

Fowler, R. H. & Nordheim, L. 1928 Electron emission in intense electric fields. *Proc. R. Soc. Lond.* A **119**, 173–181.

Fransen, M. J., van Rooy, T. L. & Kruit, P. 1999 Field emission energy distributions from individual multiwalled carbon nanotubes. *Appl. Surf. Sci.* **146**, 312–327.

Gadzuk, J. W. & Plummer, E. W. 1973 Field emission energy distributions. *Rev. Mod. Phys.* **45**, 487–584.

Gao, R., Pan, Z. & Wang, Z. L. 2001 Work function at the tips of multiwalled carbon nanotubes. *Appl. Phys. Lett.* **78**, 1757–1759.

Gomer, R. 1961 *Field emission and field ionization*. Cambridge, MA: Harvard University Press.

Good, R. H. & Mueller, E. W. 1956 Field emission. In *Handbuch der Physik* (ed. S. Fluegge), vol. 21, pp. 176–231. Springer.

Groening, O., Kuettel, O. M., Schaller, E., Groening, P. & Schlapbach, L. 1996 Vacuum arc discharges preceding high electron field emission from carbon films. *Appl. Phys. Lett.* **69**, 476–478.

Groening, O., Kuettel, O. M., Emmenegger, C., Groening, P. & Schlapbach, L. 2000 Field emission properties of carbon nanotubes. *J. Vac. Sci. Technol.* B **18**, 665–678.

Guillorn, M. A., Melechko, A. V., Merkulov, V. I., Ellis, E. D., Britton, C. L., Simpson, M. L., Lowndes, D. H. & Baylor, L. R. 2001 Operation of a gated field emitter using an individual carbon nanofiber cathode. *Appl. Phys. Lett.* **79**, 3506–3508.

Hafner, J. H., Cheung, C. L., Oosterkamp, T. H. & Lieber, C. M. 2001 High-yield assembly of individual single-walled carbon nanotube tips for scanning probe microscopes. *J. Phys. Chem.* B **105**, 743–746.

Hainfeld, J. F. 1977 Understanding and using field emission sources. *Scan. Electron Microsc.* **1**, 591–604.

Hata, K., Takakura, A. & Saito, Y. 2001 Field emission microscopy of adsorption and desorption of residual gas molecules on a carbon nanotube tip. *Surf. Sci.* **490**, 296–300.

Hawkes, P. W. & Kasper, E. 1996 Applied geometrical optics. *Principles of electron optics*, vol. II. Academic.

Iijima, S. 1991 Helical microtubulus of graphite carbon. *Nature* **354**, 56–58.

Jensen, K. L. 1999 Field emitter arrays for plasma and microwave source applications. *Phys. Plasmas* **6**, 2241–2243.

Jung, I. S., Seonghoon, L., Yoon, H. S., Sung, Y. C., Kyoung, I. & Kee, S. N. 2001 Patterned selective growth of carbon nanotubes and large field emission from vertically well-aligned carbon nanotube field emitter arrays. *Appl. Phys. Lett.* **78**, 901–903.

Jung, J. E. (and 16 others) 2002 Fabrication of triode-type field emission displays with high-density carbon-nanotube emitter arrays. *Physica* B **323**, 71–77.

Kuzumaki, T., Takamure, Y., Ichinose, H. & Horiike, Y. 2001 Structural change at the carbon-nanotube tip by field emission. *Appl. Phys. Lett.* **78**, 3699–3701.

Lee, Y. H., Jang, Y. T., Kim, D. H., Ahn, J. H. & Ju, B. K. 2001 Realization of gated field emitters for electrophotonic applications using carbon nanotube line emitters directly grown into submicrometer holes. *Adv. Mater.* **13**, 479–482.

Leopold, J. G., Zik, O., Cheifetz, E. & Rosenblatt, D. 2001 Carbon nanotube-based electron gun for electron microscopy. *J. Vac. Sci. Technol.* A **19**, 1790–1795.

Marcuccio, S., Genovese, A. & Andrenucci, M. 1997 FEEP microthruster technology status and prospects. In *Proc. 48th Int. Astronautical Federation Cong., Turin, Italy.* Paris: International Astronautical Federation.

Modi, A., Koratkar, N., Lass, E., Wei, B. & Alayan, P. M. 2003 Miniaturized gas ionization sensors using carbon nanotubes. *Nature* **424**, 171–174.

Nakayama, Y., Nishijima, H., Akita, S., Hohmura, K. I., Yoshimura, S. H. & Takeyasu, K. 2000 Microprocess for fabricating carbon-nanotube probes of a scanning probe microscope. *J. Vac. Sci. Technol.* B **18**, 661–664.

Nilsson, L., Groening, O., Emmenegger, C., Kuettel, O., Schaller, E., Schlapbach, L., Kind, H., Bonard, J. M. & Kern, K. 2000 Scanning field emission from patterned carbon nanotube films. *Appl. Phys. Lett.* **76**, 2071–2073.

Nishijima, H., Akita, S. & Nakayama, Y. 1999 Novel process for fabricating nanodevices consisting of carbon nanotubes. *Jpn. J. Appl. Phys.* **38**, 7247–7252.

Orloff, J. 1989 Survey of electron sources for high-resolution microscopy. *Ultramicroscopy* **28**, 88–97.

Paulmier, T., Balat-Pichelin, M., Le Queau, D., Berjoan, R. & Robert, J. F. 2001 Physico-chemical behavior of carbon materials under high temperature and ion radiation. *Appl. Surf. Sci.* **180**, 227–245.

Pirio, G., Legagneux, P., Pribat, D., Teo, K. B., Chhowalla, M., Amaratunga, G. A. J. & Milne, W. I. 2002 Fabrication and electrical characteristics of carbon nanotube field emission microcathodes with an integrated gate electrode. *Nanotechnology* **13**, 1–4.

Purcell, S. T., Vincent, P., Journet, C. & Binh, V. T. 2002*a* Hot nanotubes: stable heating of individual multiwall carbon nanotubes to 2000 K induced by the field-emission current. *Phys. Rev. Lett.* **88**, 105502.

Purcell, S. T., Vincent, P., Journet, C. & Binh, V. T. 2002*b* Tuning of nanotube mechanical resonances by electric field pulling. *Phys. Rev. Lett.* **89**, 276103.

Ren, Z. F., Huang, Z. P., Wang, D. Z., Wen, J. G., Xu, J. W., Wang, J. H., Calvet, L. E., Chen, J., Klemic, J. F. & Reed, M. A. 1999 Growth of a single freestanding multiwall carbon nanotube on each nanonickel dot. *Appl. Phys. Lett.* **75**, 1086–1088.

Riley, D., Mann, M., MacLaren, D. A., Dastoor, P. C., Allison, W., Teo, K. B. K., Amaratunga, G. A. J. & Milne, W. 2003 Helium detection via field ionization from carbon nanotubes. *Nano Lett.* **3**, 1455–1458.

Rinzler, A. G., Hafner, J. H., Nikolaev, P., Lou, L., Kim, S. G., Tomanek, D., Nordlander, P., Colbert, D. T. & Smalley, R. E. 1995 Unraveling nanotubes: field emission from an atomic wire. *Science* **269**, 1550–1553.

Rosen, R., Simendinger, W., Debbault, C., Shimoda, H., Fleming, L., Stoner, B. & Zhou, O. 2000 Application of carbon nanotubes as electrodes in gas discharge tubes. *Appl. Phys. Lett.* **76**, 1668–1670.

Saito, Y. & Uemura, S. 2000 Field emission from carbon nanotubes and its application to electron sources. *Carbon* **38**, 169–182.

Saito, Y., Hamaguchi, K., Hata, K., Uchida, K., Tasaka, Y., Ikazaki, F., Yumura, M., Kasuya, A. & Nishina, Y. 1997 Conical beams from open nanotubes. *Nature* **389**, 554–555.

Saito, R., Dresselhaus, G. & Dresselhaus, M. S. 1998 *Physical properties of carbon nanotubes.* London: Imperial College Press.

Saito, Y., Hata, K. & Murata, T. 2000 Field emission patterns originating from pentagons at the tip of a carbon nanotube. *Jpn. J. Appl. Phys.* **39**, L271–L272.

Schmid, H. & Fink, H. W. 1997 Carbon nanotubes are coherent electron sources. *Appl. Phys. Lett.* **70**, 2679–2680.

Semet, V., Binh, V. T., Vincent, P., Guillot, D., Teo, K. B. K., Chhowalla, M., Amaratunga, G. A. J., Milne, W. I., Legagneux, P. & Pribat, D. 2002 Field electron emission from individual carbon nanotubes of a vertically aligned array. *Appl. Phys. Lett.* **81**, 343–345.

Spindt, C. A. 1968 A thin film field emission cathode. *J. Appl. Phys.* **39**, 3504–3505.

Sugie, H., Tanemure, M., Filip, V., Iwata, K., Takahashi, K. & Okuyama, F. 2001 Carbon nanotubes as electron source in an X-ray tube. *Appl. Phys. Lett.* **78**, 2578–2580.

Swanson, L. W. & Schwind, G. A. 1997 A review of the ZrO/W Schottky cathode. In *Handbook of charged particle optics* (ed. J. Orloff), pp. 77–102. Boca Raton, FL: CRC Press.

Takakura, A., Hata, K., Saito, Y., Matsuda, K., Kona, T. & Oshima, C. 2003 Energy distributions of field emitted electrons from a multi-wall carbon nanotube. *Ultramicroscopy* **95**, 139–143.

Teo, K. B. (and 14 others) 2003 Plasma enhanced chemical vapour deposition carbon nanotubes/nanofibres—how uniform do they grow? *Nanotechnology* **14**, 204–211.

Thong, J. T. L., Oon, C. H., Yeadon, M. & Zhang, W. D. 2002 Field-emission induced growth of nanowires. *Appl. Phys. Lett.* **81**, 4823–4825.

Tiemeijer, P. C., Lin, J. H. A. & de Jong, A. F. 2001 First results of a monochromized 200 kV TEM. *Microsc. Microanalysis* **7**, 1130–1131.

van Veen, A. H. V., Hagen, C. W., Barth, J. E. & Kruit, P. 2001 Reduced brightness of the Zr/W Schottky electron emitter. *J. Vac. Sci. Technol.* B **19**, 2038–2044.

Visser, H. M., Rosink, J. J. W. M., Gillies, M. F., van der Vaart, N. C., van der Poel, W. A. J. A. & Cosman, E. C. 2003 Field emission display architecture based on hopping electron transport. In *Proc. SID 2003 Int. Symp., 20–22 May 2003, Baltimore, MD.*

Wang, Q. H., Setlur, A. A., Lauerhaas, J. M., Dai, J. Y., Seelig, E. W. & Chang, R.-P. H. 1998 A nanotube-based field-emission flat panel display. *Appl. Phys. Lett.* **72**, 2912–2913.

Wang, Z. I., Poncharal, P. & de Heer, W. A. 2000 Nanomeasurements in transmission electron microscopy. *Microsc. Microanalysis* **6**, 224–230.

Wang, Q. H., Yan, M. & Chang, R. P. H. 2001 Flat panel display prototype using gated carbon nanotube field emitters. *Appl. Phys. Lett.* **78**, 1294–1296.

Wang, Z. L., Poncharal, P. & de Heer, W. A. 2002 *In situ* imaging of field emission from individual carbon nanotubes and their structural damage. *Appl. Phys. Lett.* **80**, 856–858.

Wei, Y. Y., Dean, K. A., Coll, B. F. & Jaskie, J. E. 2001 Stability of carbon nanotubes under electric field studied by scanning electron microscopy. *Appl. Phys. Lett.* **79**, 4527–4529.

Yaguchi, T., Sato, T., Kamino, T., Taniguchi, Y., Motomiya, K., Tohji, K. & Kasuya, A. 2001 A method for characterizing carbon nanotubes. *J. Electron Microsc.* **50**, 321–324.

Yenilmez, E., Wang, Q., Chen, R. J., Wang, D. & Dai, H. 2002 Wafer scale production of carbon nanotube scanning probe tips for atomic force microscopy. *Appl. Phys. Lett.* **80**, 2225–2227.

Yu, S. G. (and 10 others) 2001 Undergate-type triode carbon nanotube field emission display with a microchannel plate. *Jpn. J. Appl. Phys.* **40**, 6088–6091.

Yu, S. G. (and 10 others) 2002 Energy distribution for undergate-type triode carbon nanotube field emitters. *Appl. Phys. Lett.* **80**, 4036–4038.

Yue, G. Z., Qiu, Q., Gao, B., Cheng, Y., Zhang, J., Shimoda, H., Chang, S., Lu, J. P. & Zhou, O. 2002 Generation of continuous and pulsed diagnostic imaging X-ray radiation using a carbon-nanotube-based field-emission cathod. *Appl. Phys. Lett.* **81**, 355–357.

Zhu, W. 2001 *Vacuum micro-electronics*. Wiley.